Chemistry
A European
Journal

Chemistry Europe
European Chemical Societies Publishing

## Accepted Article

**Title:** Quantification and Prediction of Imine Formation Kinetics in Aqueous Solution by Microfluidic NMR

**Authors:** Youzhen Zhuo, Xiuxiu Wang, Si Chen, Hang Chen, Jie Ouyang, Liulin Yang, Xinchang Wang, Lei You, Marcel Utz, Zhongqun Tian, and Xiao-Yu Cao



**To be cited as:** *Chem. Eur. J.* 10.1002/chem.202100874

**Link to VoR:** https://doi.org/10.1002/chem.202100874

WILEY-VCH

10.1002/chem.202100874

WILEY-VCH

COMMUNICATION

# Quantification and Prediction of Imine Formation Kinetics in Aqueous Solution by Microfluidic NMR

Youzhen Zhuo,[a] Xiuxiu Wang,[a] Si Chen,[a] Hang Chen,[c] Jie Ouyang,[a] Liulin Yang,[a] Xinchang Wang,*[b] Lei You,*[c] Marcel Utz,*[d] Zhongqun Tian[a] and Xiaoyu Cao*[a]

Dedication ((optional))

[a] Y.-Z Zhuo, X.-X Wang, S. Chen, J. Ouyang, Dr. L.-L Yang, Prof. Z.-Q Tian, Prof. X.-Y Cao*
State Key Laboratory of Physical Chemistry of Solid Surfaces,
Collaborative Innovation Center of Chemistry for Energy Materials
(iChEM), Key Laboratory of Chemical Biology of Fujian Province
Department of Chemistry, College of Chemistry and Chemical
Engineering, Xiamen University
Xiamen 361005 (P. R. China)
E-mail: xcao@xmu.edu.cn
[b] Dr. X.-C Wang*
School of Electronic Science and Engineering, Xiamen University
Xiamen 361005 (P. R. China)
E-mail: xcwang@xmu.edu.cn
[c] H. Chen, Prof. L. You*
State Key Laboratory of Structural Chemistry, Fujian Institute of Research on the Structure of Matter
Chinese Academy of Sciences, Fuzhou 350002, China
E-mail: lyou@fjirsm.ac.cn
[d] Prof. M. Utz*
School of Chemistry, University of Southampton, Southampton, Hampshire SO17 1BJ, United Kingdom
Email: marcel.utz@soton.ac.uk

Supporting information for this article is given via a link at the end of the document.

**Abstract:** Quantitatively predicting the reactivity of dynamic covalent reaction is essential to understand and rationally design complex structures and reaction networks. In this work, we quantified the reactivity of aldehydes and amines in various rapid imine formation in aqueous solution by microfluidic NMR. Investigation of reaction kinetics allows us to quantify the forward rate constants $k_+$ by an empirical equation, of which three independent parameters were introduced as reactivity parameters of aldehydes ($S_E$, $E$) and amines ($N$). Furthermore, these reactivity parameters were successfully used to predict the unknown forward rate constants of imine formation. Finally, two competitive reaction networks were rationally designed based on the proposed reactivity parameters. Our work has demonstrated the capability of microfluidic NMR in quantifying the kinetics of label-free chemical reactions, especially rapid reactions that complete in minutes.

Dynamic covalent chemistry (DCC)[1] has been widely applied in constructing sophisticated supramolecular structures and reaction networks.[2] The most frequently used dynamic bond is imine, which can be formed by condensation between aldehydes and amines under mild reaction conditions.[3] Precise control over both thermodynamics and kinetics of imine formation has greatly promoted the construction of complex structures and chemical systems.[3b] For instance, Cooper et al. integrated calculations and experiments to discover 32 new imine-based cages through one-pot syntheses in chloroform.[4] In aqueous system, imines are also important building blocks in constructing supramolecular structures.[5] Nevertheless, fundamental physical-organic properties of imine formation in aqueous solution need thorough study, which is a prerequisite for predicting product distributions in DCC reactions.[3b] In a simple system that just involves one amine and one aldehyde/ketone, conventional spectroscopies, such as UV-Vis and IR, successfully provide quantitative information of imine formation[6] by monitoring the absorption of imine group. However, they are limited in studying muticompent complex systems that contain multiple amine and aldehyde/ketone components, owing to the limited structural resolution of these spectroscopies.

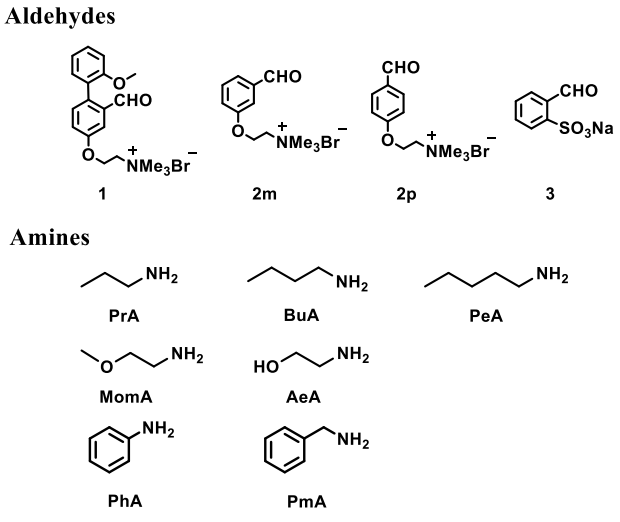


**Scheme 1.** Chemical structures of the aldehydes (1-3) and the amines (PrA-PmA) used in this work.

10.1002/chem.202100874



COMMUNICATION

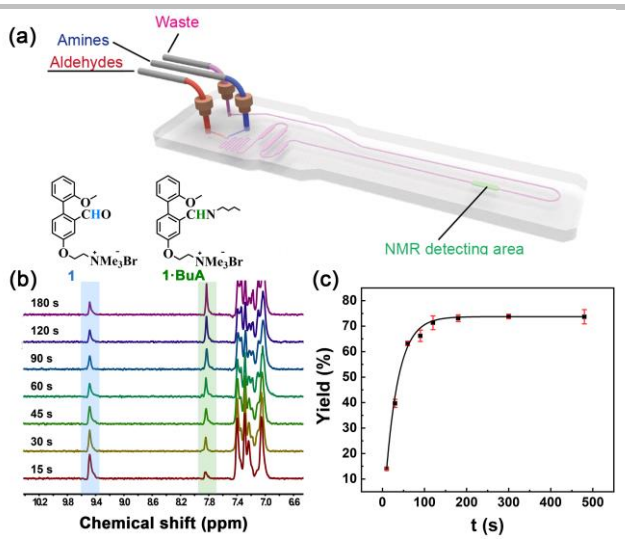


**Figure 1.** (a) Schematic diagram of fluid flow process in the microfluidic chip. (b) time-resolved $^1$H NMR spectra and (c) yield plot of reaction between **1** (10 mM) and **BuA** (10 mM) at different reaction time in $D_2O$ at 25 ℃. Error in experiments: ±5%.

Nuclear magnetic resonance (NMR) is a powerful tool to study organic reactions, because it provides valuable high-resolution structural information.[7] Over the past decade, thermodynamics and kinetics of imine formation with time scales ranging from hours to days have been investigated by conventional NMR,[8] such as the time-dependent distribution of imine reaction network[9] and the influence of weak n-π* interaction[10] in protecting imine bonds. But it fails to characterize the kinetics of aqueous imine formation finished within minutes for two reasons. First, important kinetic profiles at the early stage of reactions are missing because it takes at least 3 min to acquire the first NMR spectrum. Second, poor sensitivity of NMR requires the accumulation of scans to achieve an acceptable signal-to-noise ratio (S/N), leading to poor time resolution. The combination of flow systems with NMR[11] provides enchanced NMR-based techniques, such as flow NMR[12] and microfluidic NMR (μF-NMR),[13] which significantly improve the time resolution.[14] For instance, Wensink et al. reported the first work on monitoring the kinetics of fast imine formation using microfluidic NMR.[15] But due to the low sensitivity of the planar coil, a high concentration of reactants (4.95 M) was required. Oosthoek-de Vries et al.[16] have used a highly efficient stripline NMR flow probe to study the kinetics of fast acetylation of benzyl alcohol on a time scale of seconds at 500 mM.

Recently, our group has successfully employed microfluidic NMR (μF-NMR) to investigate the kinetics of a multi-component host-guest supramolecular system.[17] Taking the advantage of high sensitivity of double striplines in our design,[18] we have reduced the concentration of reactants to as low as 2 mM. Herein, we applied μF-NMR to characterize the kinetics of a variety of fast imine formation in aqueous solution. Time-resolved NMR spectra allow us to systematically investigate the kinetics and establish the kinetic models. We then employed an empirical equation to quantify the reactivity of aldehydes and amines. The collected parameters can be directly used to predict the forward reaction rate constant. We also designed two competitive imine-based networks based on their different reactivities and demonstrated the effect of amines and aldehydes on the kinetic and thermodynamic control. Our work has successfully quantified the reactivities of imine formation and demonstrated the capability of μF-NMR in characterizing dynamic covalent chemistry.

In our previous work, we tried to study the kinetics of imine formation in aqueous solution by conventional NMR,[10] for instance aldehyde **1** and aliphatic amines. But the reactions already finished when the first NMR spectrum was recorded at 5 min. Thus, we first mixed **1** with *n*-butylamine (**BuA**) to analyze the feasibility of monitoring imine formation in aqueous solution using μF-NMR. After injecting an aqueous solution of **1** (20 mM) and **BuA** (20 mM) into a microfluidic chip by syringe pumps (Figure 1a), the time-resolved $^1$H-NMR spectra (Figure 1b) clearly showed that the reaction finished at 180 s. As the reaction went on, the peak area of reactant ($H_{CHO}$ at 9.45 ppm) gradually decreased, whereas the peak area of product ($H_{CHN}$ at 7.8 ppm) gradually increased. Integration of those peaks was plotted to give the profile of the yield against time (Figure 1c), as well as equilibrium constant *K*. Similarly, condensation of **1** with several types of amines, such as aliphatic amine **PrA-PeA**, hydroxy or methoxy containing amine **MomA-AeA**, and aromatic amine **PhA** were also investigated (See Supporting Information, Fig. S2-11†). The kinetic curves were first fitted by a second-order equation, which is commonly used for imine formation in organic solution. Taking the condensation of **1** and **AeA** for example, no obvious linear relationship between 1/[CHO] and time was observed (Figure 2b), except for the early stage of the reaction.

We hypothesized that at the early stage, the concentration of products is quite low, and the reverse reaction rate is approximately zero. The total reaction rate equals the forward reaction rate ($r \approx r_+$), which obeys the second-order equation. As the reaction proceeds, the concentration of [CHN] together with the rate of imine hydrolysis increase, leading to the deviation from the second-order reaction process. Therefore, imine formation should be considered as a reversible reaction in aqueous solution.

$$A = -\frac{K\ln\left(2Kx + \sqrt{4KC_0 + 1} - 2KC_0 - 1\right)}{\sqrt{4KC_0 + 1}} + \frac{K\ln\left(2Kx - \sqrt{4KC_0 + 1} - 2KC_0 - 1\right)}{\sqrt{4KC_0 + 1}} = k_+ t + C \qquad (1)$$

The 2-1 reversible reaction equation **(1)** was attempted to fit the kinetics of imine formation (page S8 in Supporting Information)

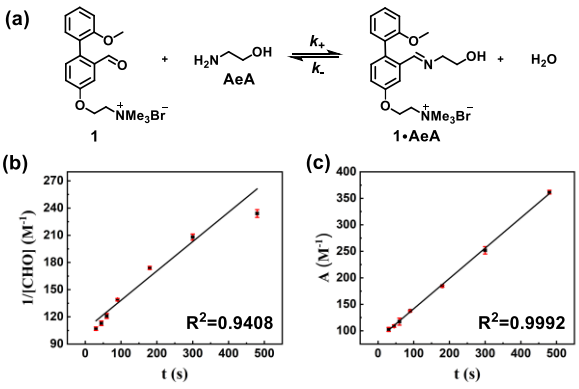


**Figure 2.** (a) The reaction of **1** with **AeA**. The plot of the fitting curve by (b) the second-order kinetic equation and (c) the 2-1 reversible kinetic equation. Error in experiments: ±5%.

10.1002/chem.202100874



# COMMUNICATION

The fitting resulted in an excellent correlation coefficient $R^2$ (0.9992) (Figure 2c). Moreover, besides $k_+$ and $K$, reverse constant $k_-$ can also be acquired by calculation. For comparison, we also introduced aldehydes **2m**, **2p,** and **3** to investigate the substituent effect on the reaction kinetic. All kinetic data were summarized in Table 1.

**Table 1.** Summary of the equilibrium constant $K$, rate constant $k_+$, and $k_-$ of imine formation.

| Aldehydes | Amines | $K$ ($M^{-1}$) [a] | $k_+$ ($M^{-1}\cdot s^{-1}$) [a] | $k_-$ ($s^{-1}$) [b] |
|---|---|---|---|---|
| 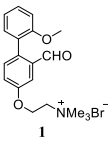 **1** |  | 568 | 2.30 | $4.05\times10^{-3}$ |
| |  | $1.07\times10^{3}$ | 3.47 | $3.24\times10^{-3}$ |
| |  | 884 | 3.32 | $3.76\times10^{-3}$ |
| |  | 361 | 0.531 | $1.47\times10^{-3}$ |
| |  | 325 | 0.291 | $8.96\times10^{-4}$ |
| |  | 14.8 | -[c] | -[c] |
| 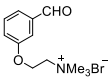 **2m** |  | 516 | 1.60 | $3.10\times10^{-3}$ |
| |  | 643 | 2.22 | $3.45\times10^{-3}$ |
| |  | 269 | 1.98 | $7.36\times10^{-3}$ |
| |  | 287 | 0.552 | $1.92\times10^{-3}$ |
| |  | 302 | 0.352 | $1.17\times10^{-3}$ |
| |  | 5.36 | -[c] | -[c] |
| 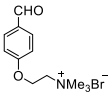 **2p** |  | 127 | 0.593 | $4.67\times10^{-3}$ |
| |  | 158 | 0.849 | $5.37\times10^{-3}$ |
| |  | 181 | 0.788 | $4.35\times10^{-3}$ |
| |  | 53.9 | 0.223 | $4.14\times10^{-3}$ |
| |  | 52.4 | 0.154 | $2.94\times10^{-3}$ |
| |  | 1.83 | -[c] | -[c] |
|  **3** |  | $2.68\times10^{3}$ | 3.74 | $1.40\times10^{-3}$ |
| |  | $4.34\times10^{3}$ | 4.56 | $1.05\times10^{-3}$ |
| |  | $3.24\times10^{3}$ | 4.37 | $1.35\times10^{-3}$ |
| |  | $2.83\times10^{3}$ | 1.39 | $4.91\times10^{4}$ |
| |  | $1.32\times10^{3}$ | 0.842 | $6.38\times10^{4}$ |
| |  | 28.3 | -[c] | -[c] |

[a] Error in experiments: ±5%. [b] Error in experiments: ±10%. [c] the concentration is below the detection limit.

**Table 2.** The values of reactivity parameter $N$ of amines.

| Amine | MomA | AeA | PrA | PeA | BuA |
|---|---|---|---|---|---|
| $N$ [a] | −1.23 | −0.63 | 0.83 | 1.20 | 1.24 |

[a] Error in experiments: ±5%.

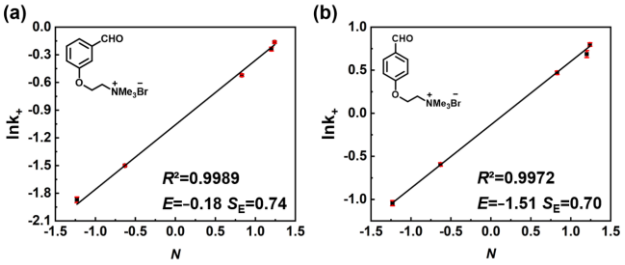


**Figure 3.** Plots of reactivity parameter $N$ versus ln$k_+$ of the reaction of (a) **2m** and (b) **2p** with amines. Error in experiments: ±5%.

We investigated the kinetics of imine formation between various aldehydes and amines, and tried to correlate to their molecular structures. The $k_+$ of four aldehydes with each amine decreased in an order of **3**>**1**>**2m**>**2p**, which is in accordance with the order of the electronic effect of substituents on the aldehydes.

Likewise, the $k_+$ of reactions of amines with each aldehyde follow an order of *n*-butylamine > *n*-pentylamine > *n*-propylamine > 2-hydroxyethylamine > 2-methoxy-ethylamine. But the $pK_a$, HOMO energy levels and electron density of these amines (Figure S43-45†) showed no linear positive correlation to their $k_+$. Therefore, the basic molecular properties ($pK_a$, HOMO energy levels and electron density) of the reactants are insufficient to predict the $r_+$.

**Table 3.** Predicted and experimental values of rate constant $k_+$ for the reactions of aldehydes and PmA.

| Amine | Aldehydes | Predicted value | Experiment value | Error |
|---|---|---|---|---|
| 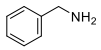 $N$=−0.35 | 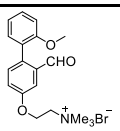 $E$=0 $S_E$=1 | - | 0.705 $M^{-1}\cdot s^{-1}$ | - |
| | 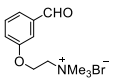 $E$= −0.18 $S_E$= 0.74 | 0.676 $M^{-1}\cdot s^{-1}$ | 0.686 $M^{-1}\cdot s^{-1}$ | 1.46% |
| | 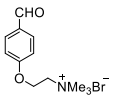 $E$= −1.51 $S_E$= 0.70 | 0.272 $M^{-1}\cdot s^{-1}$ | 0.261 $M^{-1}\cdot s^{-1}$ | 4.21% |
| |  $E$= 1.02 $S_E$= 0.67 | 1.56 $M^{-1}\cdot s^{-1}$ | 1.47 $M^{-1}\cdot s^{-1}$ | 6.12% |

10.1002/chem.202100874





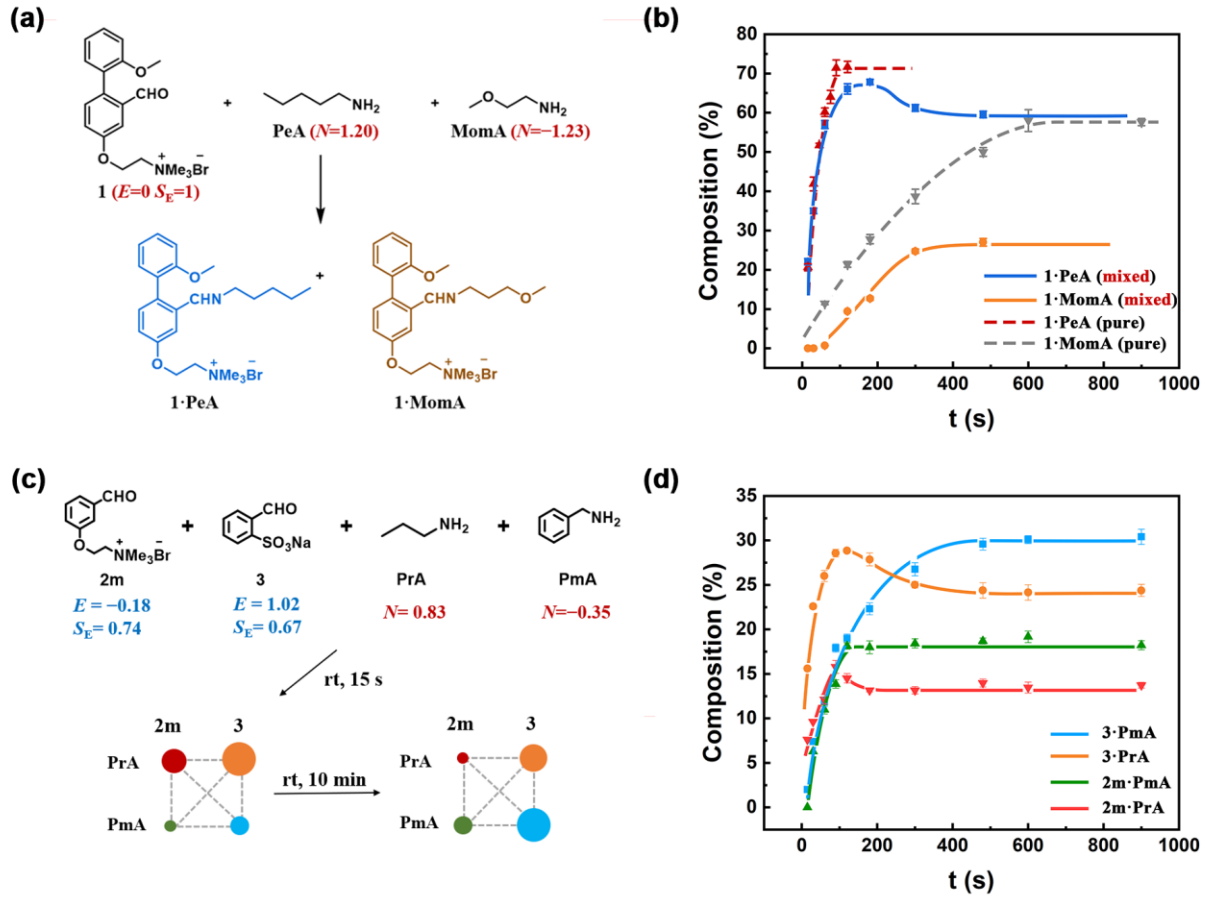


**Figure 4.** (a) Kinetic selectivity for the reaction of **1** with **PeA** and **MomA**. (b) Kinetic trace for imine formation from the reactions of aldehyde **1** with the amine **PeA** and **MomA** separately (dotted) and a mixture of the amine **PeA** and **MomA** (Solid). (c) Kinetic selectivity for the reaction of **3** and **2m** with **PrA** and **PmA**. (d) Kinetic plots of the evolution of the compounds generated from a mixture of equal amounts of components **2m** + **3** + **PrA** + **PmA** as a function of time. The size of circle means the relative content of different products. The concentration of reactants was 10 mM in all cases. Error in experiments: ±5%.

To unambiguously quantify the reaction rate constants of imine formation, we employed an empirical equation proposed by Mayr.[19] This equation relies on three basic assumptions: (1) the reactivity of amines and aldehyde are independent; (2) the reactivity of amines is defined as *N* (Nucleophilicity); (3) the aldehyde has two parameters: the reactivity of aldehyde (electrophilicity defined as *E*), and the sensitivity to amine (defined as $S_E$). Equation **(2)** was fitted with the forward reaction rate constant $k_+$ to quantify the three reactivity parameters:

$$\ln k_+ = S_E (E + N) \qquad \textbf{(2)}$$

First, aldehyde **1** was used as a reference, and its $S_E$ and *E* were assumed to be 1 and 0, respectively. Then, the reactivity parameters *N* of amines were calculated by substituting their corresponding reaction rate constants $k_+$ between **1** into the equation **(2)** (Table 2). With all the *N* of amines derived, the reactivity parameters ($S_E$ and *E*) of other aldehydes can also be quantified. The $k_+$ of aldehyde **2m** and **2p** with other amines were measured. Plotting *N* of amines against ln$k_+$ of **2m** and **2p** with these amines gave the reactivity parameters of **2m** and **2p** (Figure 3). This demonstrated the applicability of empirical equation **(2)** in quantifing experimental $k_+$ with calculated reactivity parameters, although the physical meaning of those parameters is not straightforward.

In addition, the equation **(2)** can also be used to predict the unknown experimental $k_+$ using the aforementioned reactivity parameters. Taking phenylmethanamine (**PmA**) as an example, its $k_+$ with different aldehydes were predicted using equation **(2)**. First, the **PmA** reacted with **1** to derive its reactivity parameter *N* to be −0.35. Then the $k_+$ of **PmA** with **2m**, **2p,** and **3** were calculated using equation (2), as listed in Table 3. The errors between the predicted and experimental $k_+$ were 1.46%, 4.21%, and 6.12%, respectively. Hence, equation **(2)** can predict the experimental $k_+$ of imine formation once the reactivity parameters of corresponding aldehydes or amines are derived.

Furthermore, the derived reactivity parameters of aldehydes and amines allow us to rationally design and investigate the kinetic selectivity in dynamic covalent chemistry. The designed competitive reaction system contains two amines with large difference in reactivity and an aldehyde: *n*-pentylamine (**PeA**, *N*=1.20, 10 mM) and 2-methoxy-ethylamine (**MomA**, *N*=−1.23, 10 mM), and aldehyde **1** (10 mM). As expected, at the early stage of the reaction (within 200 s), **1** reacted more quickly with **PeA** than **MomA** (Figure 4b), as the concentration of **1·PeA** reached a maximum of 66% at 200 s. This means amine with larger *N* dominates in the kinetic selection of its corresponding product. At the end of the reaction (after 200 s), the system gradually reached thermodynamic equilibrium, and due to competition from **MomA**, the ratio of **1·PeA** decreased to 58% at 480 s. Moreover, the time

for competitive system to reach its thermodynamic equilibrium is determined by the slowest process. In this case, the slower formation of **1·MomA** determines the time to reach the thermodynamic equilibrium of the system (Figure 4b). Hence, our proposed reactivity parameters can be used to design the kinetic selection. For instance, if one wants to accelerate an imine formation process, amines with large reactivity (*N*) can be introduced into the systems, vice versa.

We further designed a more complex [2×2] competitive system (Figure 4c), which contains two amines (**PrA** and **PmA**) and two aldehydes (**2m** and **3**). At the early stage of reaction (30 s), **3·PrA** formed rapidly as a major product (Figure 4d, orange), along with a small amount of **2m·PrA**. This can be explained by much higher reactivity of **PrA** (*N*=0.83) compared with **PmA** (*N*=-0.35). Thus, the kinetics of imine formation are dominated by amines rather than aldehydes, further proved the availability of reactivity parameters in designing kinetic selection of imine-based chemical reaction networks. By contrast, the ratio of the thermodynamic products is dominated by aldehydes, as evidenced by the higher ratio of **3·PmA** and **3·PrA** than **2·PmA** and **2·PrA**. This experiment provides valuable information on how to manipulate kinetic and thermodynamic selection for imine formation.

In summary, we have quantified the reactivity parameters of a series of aldehydes and amines for imine formation in aqueous solution using μF-NMR. The high time-resolution NMR spectra unambiguously gave the kinetic profiles of imine formation in aqueous solution as a 2-1 reversible reaction. More importantly, we introduced an empirical equation containing the reactivity parameters of amine (*N*) and aldehyde ($S_E$ and *E*), which can quantitatively describe their reactivity parameters. Such parameters were used to predict the forward reaction rate constants ($k_+$) of an amine (**PmA**) through only one reaction. Finally, we rationally designed two competitive imine formation systems ([1×2] and [2×2]) based on their differences in reactivity parameters. Kinetic investigation of competitive systems revealed that the kinetic selection was determined by the reactivity of amines, whereas thermodynamics distribution was determined by the stability of aldehydes. Our work demonstrated the capability of μF-NMR in studying the kinetics of fast chemical reactions, and quantification of the reactivity parameters of imine formation.

## Acknowledgements

This work is supported by the NSFC (No. 91427304, 21573181, 91227111, 21971216, 21722304, 21672214, and 21971217), the Top-Notch Young Talents Program of China, and the Fundamental Research Funds for the Central Universities of China (No. 20720160050). Xinchang Wang and Liulin Yang also thank the support from Nanqiang Young Top-notch Talent Fellowship in Xiamen University, and Lei You thanks the Key Research Program of Frontier Sciences (QYZDB-SSW-SLH030) of the CAS for funding. Development and construction of the NMR probe were supported in part by a Marie Curie Career Integration Grant to MU by the European Commission (Project μF-NMR) and by the EU H2020 Project "TISuMR".

**Keywords:** Dynamic covalent chemistry • Imines • Microfluidic NMR • Dynamic combinatorial library • Kinetics

[1] a) Y. Liu, J.-M. Lehn, A. K. H. Hirsch, *Acc. Chem. Res.* **2017**, *50*, 376-386; b) W. Zhang, Y. Jin, *Dynamic Covalent Chemistry: Principles, Reactions, and Applications*, John Wiley & Sons Ltd, Chichester, **2018**, p. 1-26; c) J. F. Reuther, S. D. Dahlhauser, E. V. Anslyn, *Angew. Chem. Int. Ed.* **2019**, *58*, 74-85; *Angew. Chem.* **2019**, *131*, 76-88.

[2] a) H. Xu, W. Cao, X. Zhang, *Acc. Chem. Res.* **2013**, *46*, 1647-1658; b) N. Giri, M. G. Del Popolo, G. Melaugh, R. L. Greenaway, K. Ratzke, T. Koschine, L. Pison, M. F. C. Gomes, A. I. Cooper, S. L. James, *Nature* **2015**, *527*, 216-220; c) J. Xia, P. Zhao, K. Zheng, C. Lu, S. Yin, H. Xu, *Angew. Chem. Int. Ed.* **2019**, *58*, 542-546; *Angew. Chem.* **2019**, *131*, 552-556.

[3] a) M. E. Belowich, J. F. Stoddart, *Chem. Soc. Rev.* **2012**, *41*, 2003-2024; b) A. J. Greenlee, C. I. Wendell, M. M. Cencer, S. D. Laffoon, J. S. Moore, *Trends Chem.* **2020**, *2*, 1043-1051.

[4] R. L. Greenaway, M. J. Bennison, B. M. Alston, C. J. Pugh, M. A. Little, E. G. B. Eden-Rump, R. Clowes, A. Shakil, H. J. Cuthbertson, H. Armstrong, M. E. Briggs, A. I. Cooper, V. Santolini, M. Miklitz, K. E. Jelfs, *Nat. Commun.* **2018**, *9*, 2849.

[5] a) A. Herrmann, *Chem. Soc. Rev.* **2014**, *43*, 1899-1933; b) Y. Lei, Q. Chen, P. Liu, L. Wang, H. Wang, B. Li, X. Lu, Z. Chen, Y. Pan, F. Huang, H. Li, *Angew. Chem. Int. Ed.* **2021**, *60*, 4705-4711; *Angew. Chem.* **2021**, *133*, 2-9.

[6] a) G. M. Santerre, C. J. Hansrote, T. I. Crowell, *J. Am. Chem. Soc.* **1958**, *80*, 1254-1257; b) W. P. Jencks, *J. Am. Chem. Soc.* **1959**, *81*, 475-481; c) E. H. Cordes, W. P. Jencks, *J. Am. Chem. Soc.* **1963**, *85*, 2843-2848; d) K. Koehler, W. Sandstrom, E. H. Cordes, *J. Am. Chem. Soc.* **1964**, *86*, 2413-2419; e) J. M. Sayer, W. P. Jencks, *J. Am. Chem. Soc.* **1973**, *95*, 5637-5649; f) M. Ciaccia, S. Di Stefano, *Org. Biomol. Chem.* **2015**, *13*, 646-654.

[7] E. Harel, L. Schroder, S. Xu, *Annu. Rev. Anal. Chem.* **2008**, *1*, 133-163.

[8] C. Godoy-Alcantar, A. K. Yatsimirsky, J. M. Lehn, *J. Phys. Org. Chem.* **2005**, *18*, 979-985.

[9] a) Y. Zhou, L. Li, H. Ye, L. Zhang, L. You, *J. Am. Chem. Soc.* **2016**, *138*, 381-389; b) S. Kulchat, M. N. Chaur, J.-M. Lehn, *Chem-Eur. J.* **2017**, *23*, 11108-11118; c) M. He, J.-M. Lehn, *J. Am. Chem. Soc.* **2019**, *141*, 18560-18569.

[10] H. Zheng, H. Ye, X. Yu, L. You, *J. Am. Chem. Soc.* **2019**, *141*, 8825-8833.

[11] a) W. P. Bula, W. Verboom, D. N. Reinhoudt, H. J. G. E. Gardeniers, *Lab Chip* **2007**, *7*, 1717-1722; b) G. S. Jeong, S. Chung, C.-B. Kim, S.-H. Lee, *Analyst* **2010**, *135*, 460-473; c) S. Mozharov, A. Nordon, D. Littlejohn, C. Wiles, P. Watts, P. Dallin, J. M. Girkin, *J. Am. Chem. Soc.* **2011**, *133*, 3601-3608; d) J. Yue, J. C. Schouten, T. A. Nijhuis, *Ind. Eng. Chem. Res.* **2012**, *51*, 14583-14609; e) Q. Tu, L. Pang, Y. Zhang, M. Yuan, J. Wang, D. Wang, W. Liu, J. Wang, *Chin. J. Chem.* **2013**, *31*, 304-316; f) C. Liu, Y. Li, B.-F. Liu, *Talanta* **2019**, *205*, 120136; g) V. Fath, P. Lau, C. Greve, N. Kockmann, T. Roeder, *Org. Process Res. Dev.* **2020**, *24*, 1955-1968.

[12] D. A. Foley, E. Bez, A. Codina, K. L. Colson, M. Fey, R. Krull, D. Piroli, M. T. Zell, B. L. Marquez, *Anal. Chem.* **2014**, *86*, 12008-12013.

[13] a) R. M. Fratila, A. H. Velders, *Annu. Rev. Anal. Chem.* **2011**, *4*, 227-249; b) V.-V. Telkki, V. V. Zhivonitko, A. Selent, G. Scotti, J. Leppaeniemi, S. Franssila, I. V. Koptyug, *Angew. Chem. Int. Ed.* **2014**, *53*, 11289-11293; *Angew. Chem.* ***2014***, *126*, 11471-11475; c) A. Bracher, S. Hoch, K. Albert, H. J. Kost, B. Werner, E. von Harbou, H. Hasse, *J. Magn. Reson.* **2014**, *242*, 155-161; d) A. Scheithauer, A. Braecher, T. Gruetzner, D. Zollinger, W. R. Thiel, E. von Harbou, H. Hasse, *Ind. Eng. Chem. Res.* **2014**, *53*, 17589-17596; e) W. Wu, H. Yi, D. Chen, R. Lu, T. Yuan, J. Chen, Z. Ni, *Microsyst. Technol.* **2014**, *20*, 419-425; f) M. V. Gomez, A. M. Rodriguez, A. de la Hoz, F. Jimenez-Marquez, R. M. Fratila, P. A. Barneveld, A. H. Velders, *Anal. Chem.* **2015**, *87*, 10547-10555; g) J. Maisch, K. Kreppenhofer, S. Buechler, C. Merle, S. Sobich, B. Goerling, B. Luy, R. Ahrens, A. E. Guber, P. Nick, *J. Plant Physiol.* **2016**, *200*, 28-34; h) M. Sharma, M. Utz, *J. Magn. Reson.* **2019**, *303*, 75-81; i) B. Wu, S. von der Ecken, I. Swyer, C. Li, A. Jenne, F. Vincent, D. Schmidig, T. Kuehn, A. Beck, F. Busse, H. Stronks, R. Soong, A. R. Wheeler, A. Simpson, *Angew. Chem. Int. Ed.* **2019**, *58*, 15372-15376; *Angew. Chem.* **2019**, *131*, 15516-15520.

[14] a) J. Bart, A. J. Kolkman, A. J. Oosthoek-de Vries, K. Koch, P. J. Nieuwland, H. Janssen, J. van Bentum, K. A. M. Ampt, F. P. J. T. Rutjes, S. S. Wijmenga, H. Gardeniers, A. P. M. Kentgens, *J. Am. Chem. Soc.* **2009**, *131*, 5014-5015; b) A. Braecher, R. Behrens, E. von Harbou, H. Hasse, *Chem. Eng. J.* **2016**, *306*, 413-421.

[15] H. Wensink, F. Benito-Lopez, D. C. Hermes, W. Verboom, H. J. G. E. Gardeniers, D. N. Reinhoudt, A. van den Berg, *Lab Chip* **2005**, *5*, 280-284.
[16]A. J. Oosthoek-de Vries, P. J. Nieuwland, J. Bart, K. Koch, J. W. G. Janssen, P. J. M. van Bentum, F. P. J. T. Rutjes, H. J. G. E. Gardeniers, A. P. M. Kentgens, *J. Am. Chem. Soc.* **2019**, *141*, 5369-5380.
[17] H. Fang, Y. Sun, X. Wang, M. Sharma, Z. Chen, X. Cao, M. Utz, Z. Tian, *Sci. China Chem.* **2018**, *61*, 1460-1464.
[18] a) G. Finch, A. Yilmaz, M. Utz, *J. Magn. Reson.* **2016**, *262*, 73-80; b) M. Sharma, M. Utz, *J. Magn. Reson.* **2019**, *303*, 75-81.
[19] H. Mayr, *Tetrahedron* **2015**, *71*, 5095-5111.

10.1002/chem.202100874

WILEY-VCH



## Table of Contents

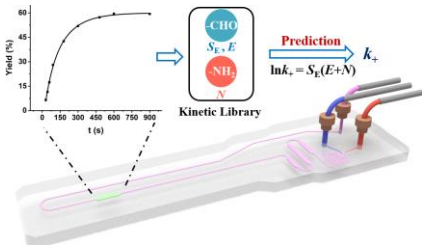


We investigated the imine formation in aqueous solution finished within several minutes through microfluidic NMR. The forward rate constants $k_+$ were quantified by an empirical equation containing three independent parameters: reactivity parameters of aldehydes ($S_E$, $E$) and amines ($N$). Those results allow the prediction of the unknown forward rate constant $k_+$ and rational design of two reaction networks exhibiting kinetic selectivity.